

# Polymer composite films and nanofibers doped with core-shell quantum dots

R. M. ABOZAIID<sup>a</sup>, D. B. STOJANOVIC<sup>a</sup>, A. RADISAVLJEVIC<sup>b</sup>, D.M. SEVIC<sup>c</sup>, M. S. RABASOVIC<sup>c</sup>,  
I. M. RADOVIC<sup>d</sup>, V. RADOJEVIC<sup>a,\*</sup>

<sup>a</sup>University of Belgrade, Faculty of Technology and Metallurgy, Belgrade, Serbia

<sup>b</sup>University of Belgrade, Innovation Center, Faculty of Technology and Metallurgy, Belgrade, Serbia

<sup>c</sup>University of Belgrade, Institute of Physics, Zemun, Serbia

<sup>d</sup>University of Belgrade, Laboratory for Materials Sciences, Institute of Nuclear Sciences "Vinča", Belgrade, Serbia

Processing and characterization of polymer nanocomposites based on poly(methyl methacrylate) (PMMA) matrix with embedded core-shell CdSe/ZnS quantum dots were investigated. Nanocomposites were obtained via solution casting and electrospinning. FESEM analysis revealed that the processing with electrospinning enables better dispersion of quantum dots. Time-resolved laser induced fluorescence measurements confirmed uniform size of QDs in fibers with the emission at only one wavelength. Oxidation effects in quantum dots were removed with the use of PMMA as a host, and the core remained active, which was confirmed with FTIR analysis and time-resolved laser induced fluorescence measurements.

(Received November 19, 2018; accepted February 17, 2020)

**Keywords:** Composite materials, Quantum dots, Electrospinning, Time-resolved optical spectroscopies

## 1. Introduction

The bare idea of highly efficient optoelectronic material brought attention to semiconductor quantum dots (QDs), which are now finding application in the new, state-of-the-art nanomaterials. By changing the size and shape of QDs, their optoelectronic properties can be successfully tailored [1-4]. Due to their ability and their photostability, they are being used for light emitting devices (LED), biosensing, fluorescent labeling, laser technology and solar cells [5-13]. Photostability of QDs can be increased with passivation of the surface, which is usually achieved by coating, i.e. by creating core-shell structure [14]. This method is well-known and proven to be successful on the example of CdSe QDs coated with ZnS [15]. Luminescence and photostability are increased because the energy band gap of CdSe falls inside ZnS band gap, thus confining the photo-generated electrons and holes in CdSe [16].

Since the wavelength of light that QDs emit depends on nanocrystal's size due to quantum confinement effect, one can control the desired emitted color by tuning the size of CdSe/ZnS. This phenomenon and various effects related to it are already being thoroughly investigated [17-20]. Sharon and co-workers presented luminescence quenching of CdSe/ZnS QDs and its possible application for DNA sensors [6]. Furthermore, optical degradation of CdSe/ZnS QDs upon gamma-ray irradiation, along with blue shift (blueing), photo-oxidation and photo-bleaching are known research topics covered so far [21-23].

These unique optical and electronic properties of core-shell QDs have opened the door for their use in polymer nanocomposites meant for sensing, membranes,

photovoltaic cells, bio-labeling and optical amplification [24, 25]. Poly(methyl methacrylate) (PMMA) is widely used as a material for optical purposes, due to its excellent optical, thermal, mechanical and chemical properties [26]. Therefore, PMMA has already been employed as a matrix material for nanocomposites with CdSe/ZnS QDs. The effects of different solvents and PMMA on QDs quantum efficiency have already been presented, and it has been established that the choice of a solvent greatly influences quantum efficiency of QDs [27]. According to previous researches, it is assumed that QDs can be uniformly dispersed within the polymer in the form of nanofibers. Agglomeration of QDs could be prevented, with the perpetuation of their optical properties, by using electrospinning technique for the processing of nanocomposites [28]. It is a well-established, simple method for the production of fine, continuous nanofibers [29-31].

This article presents luminescent and morphological properties of the electrospun PMMA-CdSe/ZnS films and nanofibers. Findings in this research can help predicting the size uniformity of core-shell QDs during the process of electrospinning, which can further be used as a tool for tuning of QDs with the goal of achieving the emission of a range of desired colors.

## 2. Experimental

Commercially available PMMA (poly(methyl methacrylate)) Acryrex® CM205 (Chi Mei Corp., Korea,  $M_w \approx 90400$  g/mol) pellets were used for a matrix material. DMF (dimethylformamide, anhydrous, 99.8 %) supplied

by Sigma-Aldrich (United States) was used as organic solvent. The core-shell CdSe/ZnS quantum dots with a mass concentration of 5mg/mL in toluene, with emission wavelength of 610 nm, were supplied from Qdparticles, Netherlands and used as received.

A 22 wt% solution of PMMA in DMF was prepared by stirring at room temperature overnight, until homogenization. The CdSe/ZnS QDs/toluene mixture with a predetermined volume (5mg/mL) was placed in an ultrasonic bath and sonicated for 5 minutes to ensure uniform dispersion of the QDs in the mixture and added to the polymer solution. The concentration of CdSe/ZnS nanoparticles in fibers was 0.06 wt%. The QDs/PMMA solution was then placed and stirred for 60 minutes to ensure dispersion of the QDs in the mixture.

One part of PMMA-QDs solution was cast into Petri dish and allowed to dry for 24 hours at room temperature and then 24 hours more at 60 °C in an oven, to eliminate residual solvent.

The rest of the solution was used to obtain fibers, which were fabricated by the electrospinning process.

The electrospinning was performed on Electrospinner CH-01, Linari Engineering, Italy, with the flow rate of 1 ml/h, 14 cm distance from collector and voltage power of 28 kV. The resulting fibers were allowed to dry for 48 hours at room temperature and then 6 hours at 50 °C in an oven. Both fibers and film were further dried for 1 hour at 50 °C in a vacuum dryer.

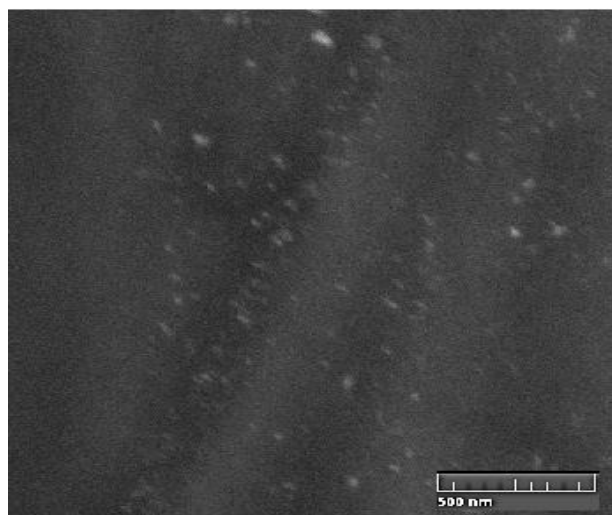
An insight of dispersion of nanoparticles was performed using FESEM (TESCAN MIRA 3) with fracture surfaces sputtered with gold. Infrared (IR) spectrums of the fibers and film were obtained with a Fourier transform infrared (FTIR) transmission-KBr disk spectroscopy (Hartmann&Braun, MB-series). Thermal analysis of composites was performed on a device for differential scanning calorimetry (DSC) in the temperature range from 24 °C to 160 °C (SDT Q600, TA instruments). The nanoindentation experiments on the powder of pure PMMA and prepared PMMA-CdSe/ZnS films and nanofibers were performed using a Triboscope T950 Nanomechanical Testing System (Hysitron, Minneapolis, MN) equipped with a Berkovich indenter type with in situ imaging mode. A peak load of 2 mN was applied for all samples with the load-hold-unload of 25s for each segment. Nine indentation measurements were performed for each sample and the mean values and standard deviations are reported. The reduced elastic modulus  $E_r$  and hardness  $H$  results were obtained by the Oliver and Pharr method [32].

The time-resolved laser induced fluorescence measurement system used in this work to investigate fluorescence of samples consists of Nd-YAG Vibrant OPO (Optical Parametric Oscillator) laser system and Hamamatsu streak camera. The OPO output used for optical excitation is tunable in the range between 320 nm and 475 nm.

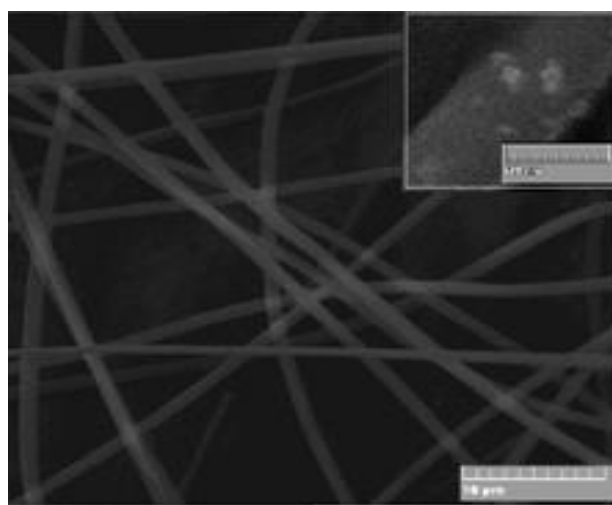
### 3. Results and discussion

FESEM photograph of PMMA-CdSe/ZnS film and nanofibers is presented in Figure 1. It can be seen that nanofibers were beads-free and with a smooth surface. Image analysis showed that over 70% of the fibers had diameters below 1  $\mu\text{m}$ . This indicates that the chosen optimal flow resulted in favorable morphology and dimensions for the use in optical devices.

Electrospinning is process for production of nano fibers from polymer solution. During drawing of solution throw nozzle viscosity and surface tension will determine stretching of the solution under electrostatic forces. The conductivity of solution is also very important. Polar DMF will increase the charges which could be carried by the jet. In this case, surface tension of solution will be easier to overcome by electrostatic charge. So, the DMF was chosen as solvent with aid to get smooth and uniform fibers [33-35].



(a)



(b)

Fig. 1. FESEM micrograph of CdSe/ZnS-PMMA (a) film and (b) fibers

Fig. 2 presents spectrums of PMMA fibers, PMMA-CdSe/ZnS fibers and film. The bands appearing in the

regions 3000–2850  $\text{cm}^{-1}$ , 1490–1275  $\text{cm}^{-1}$  and 910–750  $\text{cm}^{-1}$  of all the spectrums, originate from different  $\text{CH}_3$  and  $\text{CH}_2$  vibrational modes [35]. Bands at 1737  $\text{cm}^{-1}$  in spectrums are assigned to the stretching of C=O groups from PMMA. While spectrum of fibers PMMA-CdSe/ZnS shows absence of C=O peak coming from amide, spectrums of PMMA and PMMA-CdSe/ZnS films show peak at 1647  $\text{cm}^{-1}$ , indicating that they were not completely dry. Vibrational bands at 1450 and 991  $\text{cm}^{-1}$ , that belong to O- $\text{CH}_3$  stretching and bending deformation of PMMA, respectively, also appear in all the spectrums, along with the band at 1065  $\text{cm}^{-1}$ , ascribed to the C-O stretching vibration.

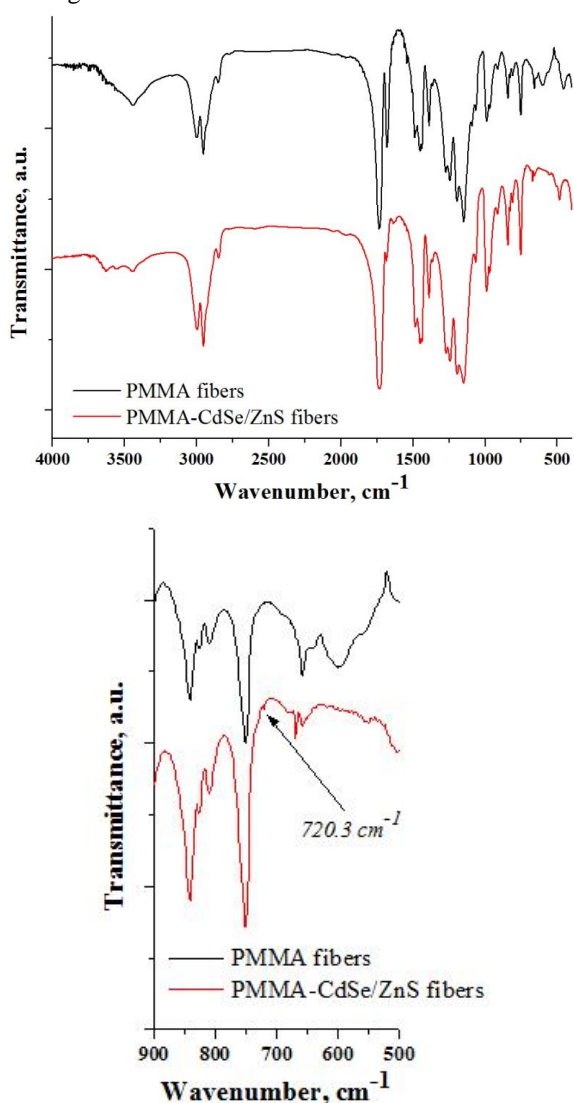


Fig. 2. FTIR spectrum of fibers and film (color online)

These findings lead to the assumption that there was no formation of a new bond between quantum dots and a host material PMMA. The most prominent peak for this research appeared at 720  $\text{cm}^{-1}$  in the spectrums of PMMA-CdSe/ZnS fibers and film, indicating the presence of CdSe active core. ZnS bond has been identified with the presence of the peak at 617  $\text{cm}^{-1}$  [36]. These results lead to the conclusion that luminescent properties of the QDs

could be preserved during the processing of the film by solution casting or fibers by electrospinning.

The results of DSC analysis are given in the Fig. 3. The analyses were performed on the powder of pure PMMA, PMMA films and nanofibers and PMMA-QD films and nanofibers. The powder of PMMA shows  $T_g$  at around 113  $^{\circ}\text{C}$ . It is obvious that there was influence of solvents in both PMMA and PMMA-QD films, decreasing  $T_g$  by 22% for PMMA and nearly 26% for PMMA-QD film. There is also a typical glass transition shoulder about 55  $^{\circ}\text{C}$  in DSC curve for PMMA-QD film, which reflects a weaker interaction between residual toluene molecules and PMMA [37, 38]. It can be noticed that the PMMA-DMF interaction is stronger in dried films because the reactions observed in that process have changed the structural characteristics of the PMMA. Opposing to the casting of films, electrospinning method gave fibers with approximately the same  $T_g$  as pure powder. This is correlated to the viscosity/polarity-dependent behavior of polymer molecules in solvent [37-39]. As Figure 3 shows, there is even a slight increase, which only further suggests that this is an appropriate technique for processing of PMMA-QD nanocomposites.

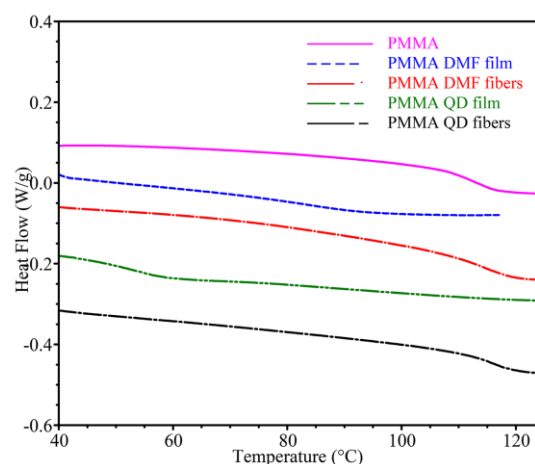


Fig. 3. DSC curves (color online)

Beside of more efficient removal of residual solvent, electrospinning ensures better dispersion of nanoparticles, hence the preservation of thermal stability of nanocomposite.

Table 1. Results of DSC analysis

Sample	$T_g$ , $^{\circ}\text{C}$
PMMA	113
PMMA/ DMF film	84
PMMA- CdSe/ZnS/ DMF film	89
PMMA/ DMF fibers	114
PMMA – CdSe/ZnS/ DMF fibers	116

Fig. 4 and Table 2 present the results obtained from nanoindentation test. Fig. 4 a) shows typical force–depth curves obtained in the nanoindentation tests for neat PMMA film and composites with CdSe/ZnS. The curves appear to be with continuity and without pop-in or pop-out in both loading and unloading phases. Figure 4 b) displays in-situ imaging mode used for scanning the surface trace that reveals the absence of cracks and fractures around the indent.

As it can be seen, with the addition of 0.06 wt% of QDs, reduced modulus increased by 6% for PMMA-

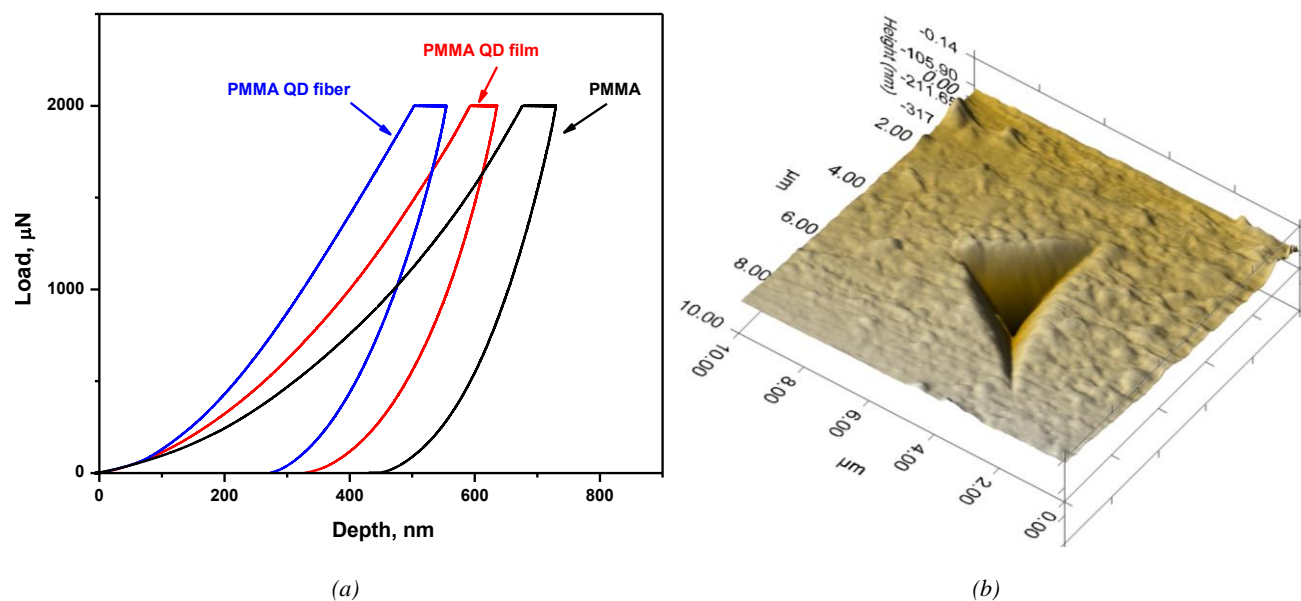


Fig. 4. Nanoindentation results (color online)

Streak image of fluorescence spectrum of CdSe/ZnS QDs liquid solution excited at 360 nm is shown in Fig. 5. The solution was prepared using one part of CdSe/ZnS toluene solution (as received) and six parts of DMF. Our aim was to check the influence of adding the DMF solvent to QDs, because PMMA host for QDs was prepared using DMF as solvent.

CdSe/ZnS films and by 23% for PMMA-CdSe/ZnS fibers, compared to pure PMMA films.

Hardness values followed the same trend as reduced modulus, increasing by 24% for films and 39% for fibers, compared to PMMA films. These results imply that the better dispersion of QD-s was achieved with electrospinning, because the mechanical properties of nanocomposites are strongly dependent of deagglomeration of nanoparticles.

Slight red shift from 610 nm (corresponding to the CdSe/ZnS QDs solution as received) to 630 nm could be observed. The analysis of CdSe/ZnS QDs hosted in PMMA dissolved in three different solvents (chloroform, toluene and tetrahydrofuran) was reported, however the wavelength shifts are smaller compared to our results [40]. The fluorescence lifetime based on the time resolved spectrum of the CdSe/ZnS QDs liquid solution is also presented in Fig. 5. The value of about 2.4 ns was obtained, which is much shorter than the values obtained in the previous researches [23].

Table 2. Results of nanoindentation test.

	E, GPa	St.dev. GPa	H, GPa	St.dev. GPa
PMMA	5.53	0.32	0.33	0.022
PMMA-CdSe/ZnS film	5.85	0.21	0.41	0.028
PMMA-CdSe/ZnS fibers	6.81	0.25	0.46	0.041

Fig. 6 shows streak images of fluorescence spectra of CdSe/ZnS QD/PMMA composite film excited at 330, 350 and 370 nm.

For all excitation wavelengths the fluorescence emission is grouped into two wide bands, around 440 nm

and 620 nm. It is easy to see that the band around 440 nm has longer fluorescence lifetime.

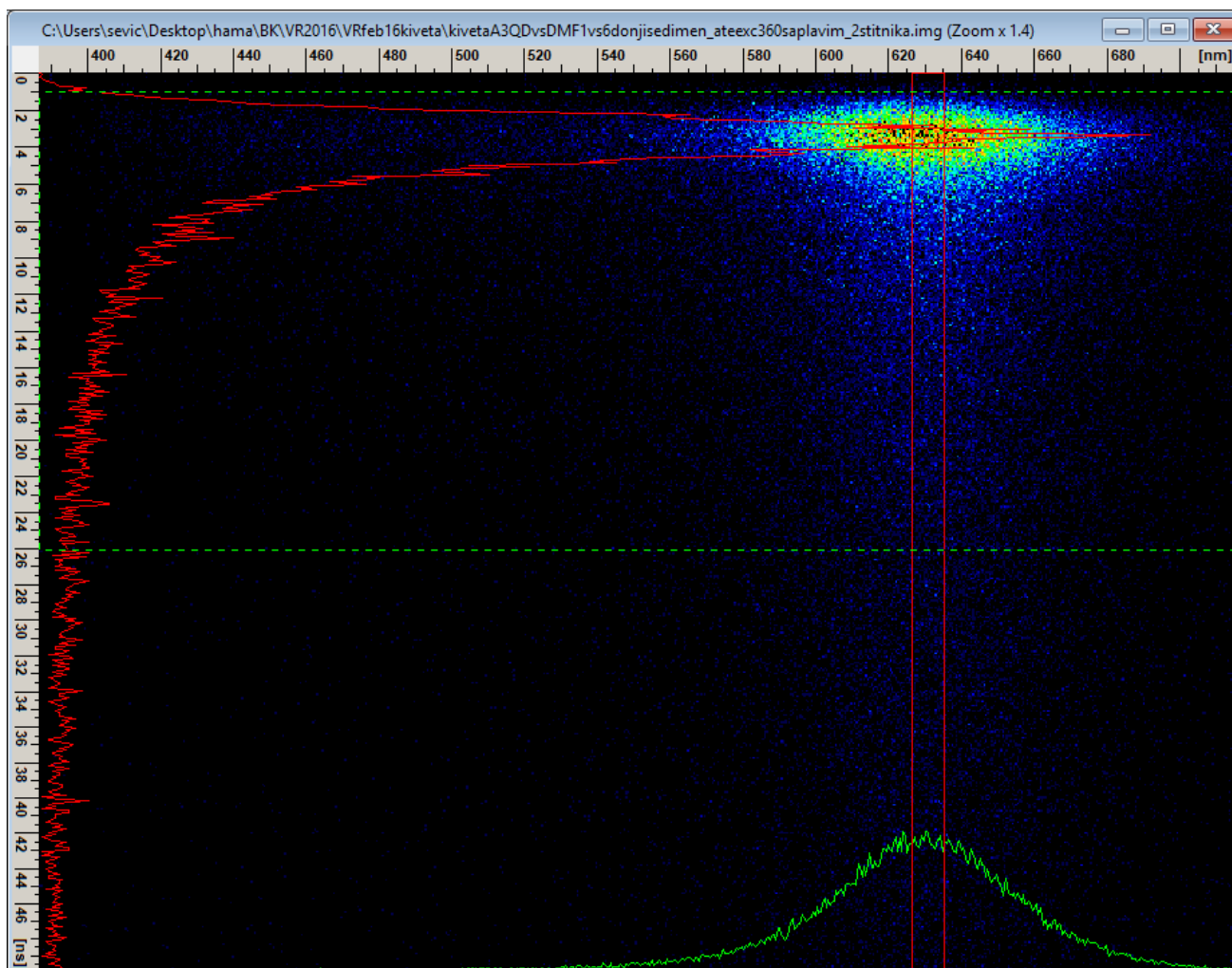


Fig. 5. Streak image of fluorescence spectrum of CdSe/ZnS QDs liquid solution excited at 360 nm (color online)

Calculated fluorescence lifetime for band around 440 nm is 6.9 ns, much longer than the lifetime of QDs liquid solution. Fluorescence lifetime of band around 620 nm is about 1.6 ns, shorter than the lifetime of QDs liquid solution. Intensity ratio of these two bands depends on excitation wavelength.

When excitation wavelength increases the band around 620 nm becomes more pronounced, while the band around 440 nm diminishes. Comparing with the values

provided in the literature [17-20], estimated core sizes of QDs embedded in PMMA after nanocomposite fabrication process are about 2.4 nm and 5.1 nm, corresponding to the detected bands around 440 nm and 620 nm, respectively.

Emission intensity as a function of illumination time of PMMA-CdSe/ZnS composite film is shown in Fig. 7.

The pulsed OPO has frequency of 10 Hz, energy of a pulse is about 5 mJ, and estimated diameter of illuminated spot is about 100  $\mu\text{m}$ .

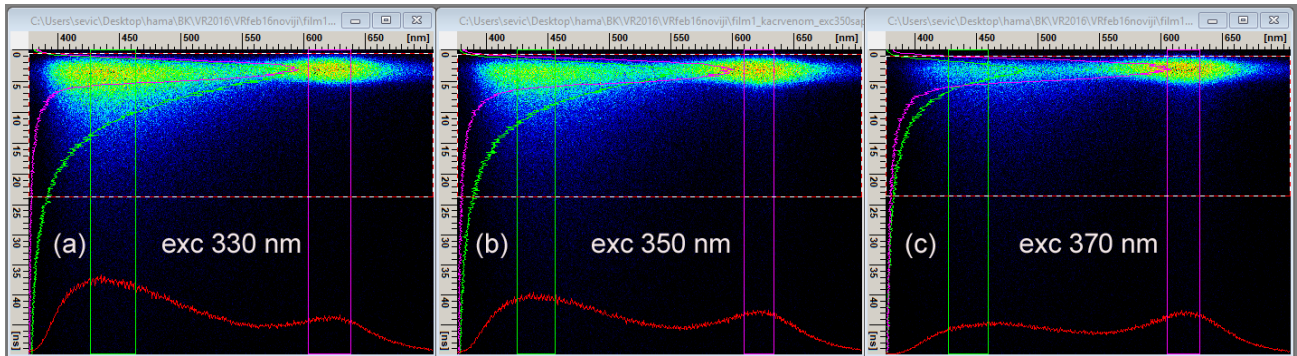


Fig. 6. Streak images of fluorescence spectra of PMMA-CdSe/ZnS composite film excited at (a) 330 nm, (b) 350 nm and (c) 370 nm (color online)

Because QDs are embedded in PMMA, there are no oxidation effects and there are no spectral shifts caused by illumination [22, 23]. Decrease of emission intensity is easy to notice, however, it seems that the bleaching effects of QDs embedded in PMMA evolve slower compared to measurements performed in nitrogen ambient.

Streak image of fluorescence spectrum of nanofibers excited at 360 nm is shown in Fig. 8.

For all excitation wavelengths the fluorescence emissions look similar, with only one very wide band. Fluorescence lifetime of PMMA-CdSe/ZnS nanofibers optical emission is about 2.2 ns, similar to the lifetime of

QDs liquid solution. Again, comparing with the values provided in the literature [17-20], estimated core size of QDs embedded in PMMA nanofibers, after the fabrication process which includes the electrospinning technique, are about 2.4 nm.

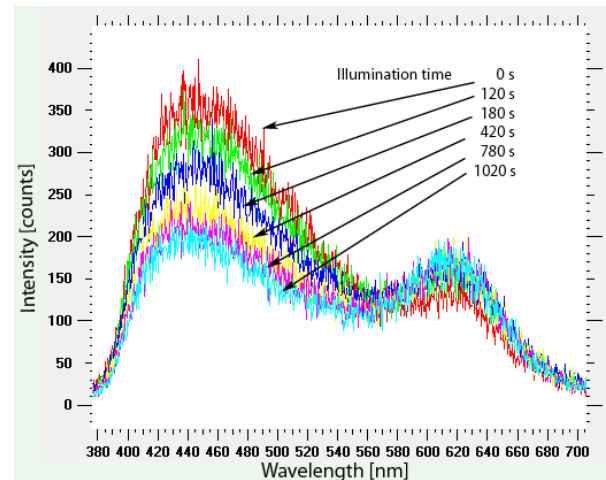


Fig. 7. Emission intensity as a function of illumination time of composite film, excited at 360 nm (color online)

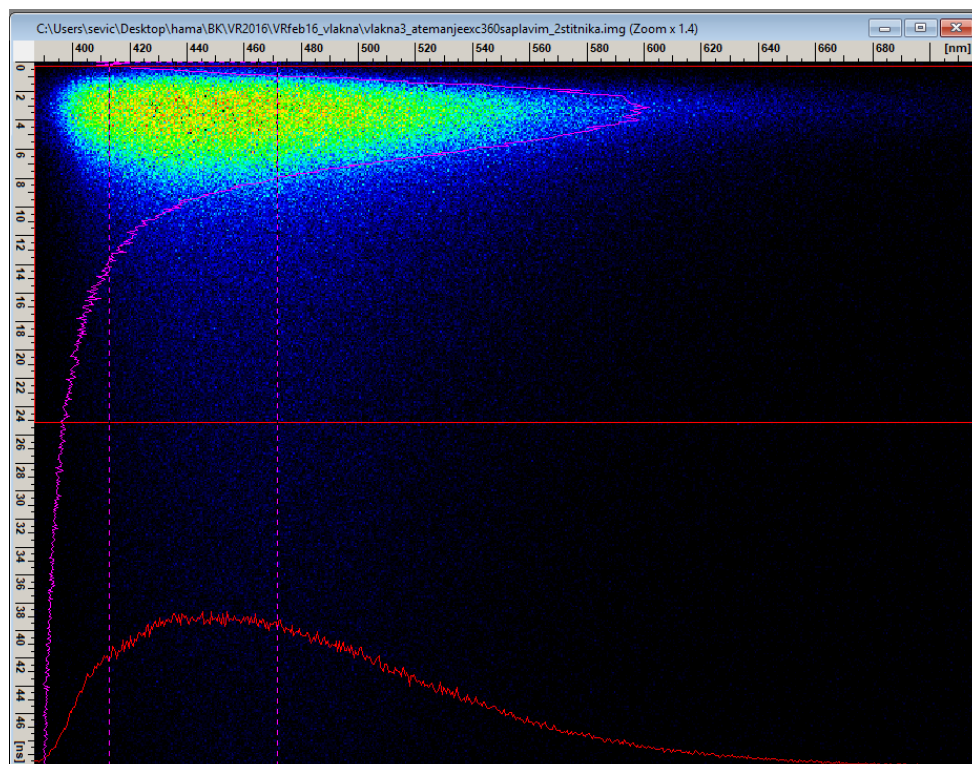


Fig. 8. Streak image of fluorescence spectrum of PMMA-CdSe/ZnS nanofibers excited at 360 nm (color online)

#### 4. Conclusion

Core-shell quantum dots CdSe/ZnS were embedded in PMMA via electrospinning and solution casting methods. PMMA has proved to be an excellent host for quantum dots, securing the preservation of their optical properties during processing. Low content of QDs was used, only 0.06 wt%, in order to show that with such concentration sufficient signal strength could be achieved. FESEM provided an insight in the morphology of fibers, and it has indicated the absence of the agglomerates. FTIR analysis revealed that the structure of QDs has remained intact, with the existence of identifying bonds coming from CdSe/ZnS in fibers and films. DSC analysis confirmed that the particles do not disrupt thermal properties of PMMA, while nanoindentation tests showed their positive impact on reduced modulus and hardness. The time-resolved laser induced fluorescence revealed that the optical activity of QD is preserved in composite films and nanofibers. Fluorescence like nanoindentation also indicates that better dispersion of QD was obtained with electrospinning method, as promising technique for processing of QD-PMMA nanocomposites with preserved optical activity of core-shell QDs.

#### Acknowledgments

This work was supported by the Ministry of Education, Science and Technological Development of the Republic of Serbia, Projects No. TR 34011 and OI 171020.

#### References

- [1] I. Gerdova, A. Haché, *Opt. Commun.* **246**, 205 (2005).
- [2] U. Woggon, *J. Appl. Phys.* **101**, 081727 (2007).
- [3] B. Bhattacharjee, C. H. Hsu, C. H. Lu, W. H. Chang, *Physica E* **33**, 388 (2006).
- [4] V. I. Klimov, S. A. Ivanov, J. Nanda, M. Achermann, I. Bezel, J. A. McGuire, A. Piryatinski, *Nature* **447**(24), 441 (2007).
- [5] D. Vasudevan, Rohit Ranganathan Gaddam, Adrian Trinchì, Ivan Cole, *J. Alloy Compd.* **363**, 395 (2015).
- [6] E. Sharon, R. Freeman, I. Willner, *Anal. Chem.* **82**, 7073 (2010).
- [7] I. L. Medintz, H. T. Uyeda, E. R. Goldman, H. Mattoussi, *Nat. Mater.* **4**, 435 (2005).
- [8] R. Bakalova, Z. Zhelev, I. Aoki, H. Ohba, Y. Imai, I. Kanno, *Anal. Chem.* **78**, 5925 (2006).
- [9] H. Kobayashi, Y. Hama, Y. Koyama, *Nano Lett.* **7**, 1711 (2007).
- [10] Y. Chan, J. Steckel, P. Snee, J. Caruge, J. Hodgkiss, D. Nocera, M. G. Bawendi. *Appl. Phys. Lett.* **86**, 0731021 (2005).
- [11] Z. Tan, F. Zhang, T. Zhu, J. Xu, A. Y. Wang, J. D. Dixon, L. Li, Q. Zhang, S.E. Mohny, J. Ruzyllo, *Nano Lett.* **7**, 3803 (2007)
- [12] I. Gur, N. A. Fromer, M. L. Geier, A. P. Alivisatos, *Science* **310**, 462 (2005).
- [13] B. S. Sun, J. Henry, A. S. Dhoot, S. G. Westenhoff, C. Neil, *J. Appl. Phys.* **97**, 014914 (2005).
- [14] D. Esparza, G. Bustos-Ramirez, R. Carriles, T. Lopez-Luke, I. Zarazua, A. Martinez-Benitez, A. Torres-Castro, E. De la Rosa, *J. Alloy Compd.* **728**, 1058 (2017).
- [15] J. Weaver, R. Zakeri, S. Aouadi, P. Kohli, J. Mater. Chem. **19**(20), 3198 (2009).
- [16] S. Mohan, O. S. Oluwafemi, S. P. Songca, S. C. George, P. Miska, D. Rouxel, N. Kalarikkal, S. Thomas, *Mat. Sci. Semicon. Proc.* **39**, 587 (2015).
- [17] V. Pilla, L. P. Alves, M. T. T. Pacheco, E. Munin, *Opt. Commun.* **281**, 5925 (2008).
- [18] L. P. Alves, V. Pilla, D. O. A. Murgo, E. Munin, *J. Dent.* **38**, 149 (2010).
- [19] B. O. Dabbousi, J. Rodriguez-Viejo, F. V. Mikulec, J. R. Heine, H. Mattoussi, R. Ober, K. F. Jensen, M. G. Bawendi, *J. Phys. Chem. B* **101**, 9463 (1997).
- [20] V. Pilla, L. P. Alves, A. N. Iwazaki, A. A. Andrade, A. Antunes, E. Munin, *Appl. Spectrosc.* **67**, 997 (2013).
- [21] R. Z. Stodilka, J. J. L. Carson, K. Yu, Md. B. Zaman, C. Li, D. Wilkinson, *J. Phys. Chem. C* **113**, 2580 (2009).
- [22] W. G. J. H. M. van Sark, P. L. T. M. Frederix, D. J. Van den Heuvel, H. C. Gerritsen, A. A. Bol, J. N. J. van Lingen, C. de Mello Donegá, A. Meijerink, *J. Phys. Chem. B* **105**, 8281 (2001).
- [23] W. G. J. H. M. van Sark, P. L. T. M. Frederix, A. A. Bol, H. C. Gerritsen, A. Meijerink, *Blueing, Chemphyschem.* **3**, 871 (2002).
- [24] L. Liu, Q. Peng, Y. Li, *Inorg. Chem.* **47**, 5022 (2008).
- [25] I. Suarez, H. Gordillo, R. Abargues, S. Albert, J. Mart, I. Pastor, *Nanotechnology* **22**, 435202 (2011).
- [26] R. M. Dukali, I. Radovic, D. B. Stojanovic, P. S. Uskokovic, N. Romcevic, V. Radojevic, R. Aleksic, *J. Alloy Compd.* **583**, 376 (2014).
- [27] H. Song, S. Lee, *Nanotechnology* **18**, 055402 (2007).
- [28] A.-M. Alam, Y. Liu, M. Park, S.-J. Park, H.-Y. Kim, *Polymer* **59**, 35 (2015).
- [29] Z. M. Huang, Y. Z. Zhang, M. Kotaki, S. Ramakrishna, *Compos. Sci. Technol.* **63**, 2223 (2003).
- [30] A. Frenot, I. S. Chronakis, *Curr. Opin. Colloid In.* **8**, 64 (2003).
- [31] L. Daelemans, S. van der Heijden, I. De Baere, H. Rahier, W. Van Paeppegem, K. de Clerck, *Compos. Sci. Technol.* **117**, 244 (2015).
- [32] W. C. Oliver, G. M. Pharr, *J. Mater. Res.* **7**, 1564 (1992).
- [33] C. Hsu, S. Shivkumar, *Macromol Mater Eng.* **289**(4), 334 (2004).
- [34] T. Jarusuwannapoom, W. Hongrojjanawiwat, S. Jitjaicham, L. Wannatong, M. Nithitanakul,

- C. Pattamaprom, P. Koombhongse, R. Rangkupan, P. Supaphol, *Eur. Pol. J* **41**(3), 409 (2005).
- [35] R. M. Dukali, I. M. Radović, D. B. Stojanović, D. M. Šević, V. J. Radojević, D. M. Jocić, R. R. Aleksić, *J. Serb. Chem. Soc.* **79**, 867 (2014).
- [36] S. Ummartyotin, N. Bunnak, J. Juntaro, M. Sain, H. Manuspiya, *Solid State Sci.* **14**, 299 (2012).
- [37] N. Patra, A. C. Barone, M. Salerno, *Adv Pol Tech.* **30**(1), 12 (2011).
- [38] M. Eriksson, H. Goossens, T. Peijs, *Nanocomposites* **1**, 36 (2015).
- [39] S. S. Musbah, V. Radojević, I. Radović, P. S. Uskoković, D. B. Stojanović, M. Dramićanin, R. Aleksić, *J. Min. Metall. Sect. B-Metall.* **48**, 309 (2012).
- [40] V. Pilla, L. P. Alves, E. Munin, M. T. T. Pacheco, *Opt. Commun.* **280**, 225 (2007).

---

\*Corresponding author: vesnar@tmf.bg.ac.rs